AIP | Journal of Applied Physics

Ferroelastic aspects of relaxor ferroelectric behaviour in Pb(In1/2Nb1/2)O3-Pb(Mg1/3Nb2/3)O3-PbTiO3 perovskite

Guillaume F. Nataf, Qian Li, Yun Liu, Ray L. Withers, Sarah L. Driver et al.

Citation: J. Appl. Phys. **113**, 124102 (2013); doi: 10.1063/1.4794027
View online: http://dx.doi.org/10.1063/1.4794027
View Table of Contents: http://jap.aip.org/resource/1/JAPIAU/v113/i12
Published by the American Institute of Physics.

JOURNAL OF APPLIED PHYSICS **113**, 124102 (2013)

Ferroelastic aspects of relaxor ferroelectric behaviour in $Pb(In_{1/2}Nb_{1/2})O_3$-$Pb(Mg_{1/3}Nb_{2/3})O_3$-$PbTiO_3$ perovskite

Guillaume F. Nataf,[1,2,a)] Qian Li,[3] Yun Liu,[3] Ray L. Withers,[3] Sarah L. Driver,[2] and Michael A. Carpenter[2]
[1]*INP Grenoble, 38031 Grenoble Cedex 1, France*
[2]*Department of Earth Sciences, University of Cambridge, Downing Street, Cambridge CB2 3EQ, United Kingdom*
[3]*Research School of Chemistry, Building 35, Australian National University, Canberra ACT 0200, Australia*

(Received 24 December 2012; accepted 18 February 2013; published online 25 March 2013)

Elastic and anelastic properties of poled and depoled single crystals of $Pb(In_{1/2}Nb_{1/2})O_3$-$Pb(Mg_{1/3}Nb_{2/3})O_3$-$PbTiO_3$ with compositions close to the morphotropic boundary have been investigated over the temperature range 5–700 K by resonant ultrasound spectroscopy (RUS) at frequencies of 0.1–1.2 MHz. Steep elastic softening occurs in a temperature interval of at least 250 K as the Vogel-Fulcher freezing interval and cubic → tetragonal transition point, T_c, are approached from above. This is understood in terms of coupling between acoustic modes and central peak mode(s) associated with dynamic polar nano regions (PNR's) below the Burns temperature. Acoustic losses occur in a temperature interval of ~50 K above T_c, associated with slowing down of the PNR dynamics. The cubic ↔ tetragonal and tetragonal ↔ rhombohedral transitions are accompanied by steep minima in elastic properties, closely analogous to the pattern of softening and stiffening observed in sequences of improper ferroelastic transitions in other perovskites. Variations in the magnitudes of acoustic losses at $T < T_c$ correlate with the density of ferroelastic twin walls, from lowest for $[001]_c$-poled and $[111]_c$-poled crystals in the stability fields of the tetragonal and rhombohedral phases, respectively, to highest for unpoled crystals. A simple model of Debye-like peaks in acoustic loss near 100 K has yielded activation energies and attempt frequencies in the same range as those observed from dielectric data in the Vogel-Fulcher freezing interval. These highlight the fact that, in addition to conventional ferroelectric/ferroelastic twin walls, relaxor ferroelectrics contain local structural heterogeneities coupled to strain, which are probably related to the presence of static PNR's preserved even in poled crystals. RUS also provides a convenient and effective means of determining the mechanical quality factor of relaxor ferroelectrics, as functions of both poling history and temperature. © *2013 American Institute of Physics*. [http://dx.doi.org/10.1063/1.4794027]

I. INTRODUCTION

Relaxor based ferroelectric single crystals with compositions in binary systems, such as $Pb(Mg_{1/3}Nb_{2/3})O_3$-$PbTiO_3$ (PMN-PT) and $Pb(Zn_{1/3}Nb_{2/3})O_3$-$PbTiO_3$ (PZN-PT), or ternary compositions, such as $Pb(In_{1/2}Nb_{1/2})O_3$-$Pb(Mg_{1/3}Nb_{2/3})O_3$-$PbTiO_3$ (PIN-PMN-PT), have been a focus of intense interest over the last 15 years, due to their ultrahigh piezoelectric performance (e.g., Refs. 1–7). The most promising phases, in terms of thermal stability, physical properties, and stability with respect to depoling, appear to have compositions near but just to the rhombohedral side of the morphotropic boundary.[8] A further refinement for controlling and optimising these properties has been to vary the configuration of macroscopic twin domains by poling along different crystallographic axes (e.g., Refs. 3–5, 8–11). For example, poling of a rhombohedral crystal at room temperature along $[001]_c$, with respect to crystallographic axes of the parent cubic structure, gives four ⟨111⟩ domains (4R), poling along $[111]_c$ gives a single rhombohedral domain state (1R) and poling along $[011]_c$ gives two rhombohedral domains (2R) (e.g., Refs. 6 and 9). Crystals with different twin configurations have different macroscopic responses to an applied stress or electric field and different resistance to becoming depoled. The presence of twin walls may or may not be beneficial, however, because their motion under the influence of an ac electric field or of a dynamic stress can give rise to significant dielectric and acoustic loss (e.g., Refs. 3, 5, 6, 8, and 10). Underlying almost all aspects of the structure/chemistry/property relationships which might be harnessed in this context are the fundamental role of phase transitions, the properties of twin walls, which may be ferroelectric, ferroelastic, or both, and the influence of static and dynamic polar nano regions (PNR's).

The zone centre soft optic mode in a conventional ferroelectric such as $PbTiO_3$ typically gives rise to a first order structural phase transition between the parent (cubic) paraelectric phase and a ferroelectric product at the Curie temperature, T_c.[12] The dielectric permittivity has a sharp maximum at temperature T_m, which is coincident with T_c and independent of measuring frequency. In the limiting case of a relaxor such as PMN, cubic lattice geometry is maintained down to low temperatures during cooling in zero field. Instead of the development of long range order at a discrete phase transition, dynamic PNR's appear below the

a)Author to whom correspondence should be addressed. Electronic mail: guillaume.nataf@phelma.grenoble-inp.fr.

Burns temperature, T_B, and there is a freezing interval marked by broad frequency-dependent maxima in the real part of the permittivity. This process involves a wide spectrum of relaxation times, which can be described in terms of Vogel-Fulcher dynamics (e.g., Refs. 13 and 14, and many references in recent reviews, such as Refs. 15 and 16). A characteristic feature of binary and ternary perovskite relaxor-ferroelectrics is that they exhibit aspects of both limiting behaviours. In particular, frequency-dependent maxima in the dielectric permittivity, relating to the collective freezing behaviour, may occur at a temperature above the temperature at which a discrete change in symmetry would be expected to occur by development of long range order ($T_m > T_c$) (e.g., Refs. 15, 17, and 18). A diffuse relaxor-ferroelectric transition occurs for $T_c \ll T_m$, though this becomes sharp if $T_c \rightarrow T_m$ (Ref. 19) (see Fig. 9 of Ref. 15). Poled crystals of relaxor ferroelectrics are also not quite the same as conventional ferroelectrics because of the persistence of static PNR's, which are themselves poled to some extent.[15] For example, in the case of PZN, static PNR's with $[110]_c$-type polarisations remain embedded within crystals, which have long-range ferroelectric order induced by an electric field applied parallel to $[111]_c$.[20] According to Xu *et al.*, "even a huge external electric field cannot remove the PNR's or force them to merge into the surrounding lattice." The static, poled PNR's form pancake-shaped regions in the stability field of the rhombohedral structure of PZN-PT (e.g., Refs. 21–23). This poling of the PNR's may also persist well into the stability field of the cubic phase.[24]

By far and away the most commonly applied technique used for characterising the properties and behaviour of both relaxor and conventional ferroelectrics is dielectric spectroscopy. The real part of the dynamic response to an ac electric field is the permittivity, ε', and the imaginary part, ε'', gives the dielectric loss as $\tan\delta = \varepsilon''/\varepsilon'$. However, because there is strong coupling between lattice distortions (strain) and the ferroelectric order parameter, it is inevitable that there will be changes in elastic and anelastic properties associated with the discrete phase transitions, the mobility of twin walls and the evolution of PNR's. Mechanical spectroscopy can, therefore, provide additional insights into the structural evolution from a slightly different perspective (for example PMN-PT[25–33]). The real part of the elastic response to a dynamic stress field, expressed as the elastic compliance, is analogous to the dielectric permittivity, and the imaginary part of the response gives the inverse mechanical quality factor, Q^{-1}, which is analogous to $\tan\delta$. Different results from dielectric and mechanical spectroscopies will be due, at least in part, to the fact that electric dipole interactions are expected to be relatively strong and short ranging in comparison with elastic strain fields, which are expected to be weaker but longer ranging. Dielectric and acoustic loss behaviour will differ also due to the fact that there is no strain contrast across twin walls between 180° domains, while twin walls between 90° domains in a tetragonal structure (109°/71° domains in a rhombohedral structure) are both ferroelectric and ferroelastic. The former will provide the main extrinsic response to an applied electric field while the latter will provide the dominant extrinsic response to a stress field.

The primary objective of the present study was to investigate strain coupling in a typical relaxor ferroelectric by observing the elastic and anelastic behaviour of poled single crystals of PIN–PMN–PT. This has been achieved across a wide temperature interval using resonant ultrasound spectroscopy (RUS), with a particular focus on the dynamical behaviour of PNR's and ferroelastic twin walls. There are a number of different ways of measuring elastic properties but RUS provides a convenient method for following elastic relaxations in the frequency range ~0.1–2 MHz. Recent studies of phase transitions in improper ferroelastic perovskites such as $SrZrO_3$,[34] $BaCeO_3$,[35] $PrAlO_3$,[36] $LaAlO_3$,[37] $KMnF_3$,[38] for example, all display marked changes in elastic properties due to strain/order parameter coupling, while the dynamics of transformation-related microstructures can be followed through the evolution of Q. The same approach to PMN has revealed an increase in elastic compliance which mimics that of ε' through the freezing interval and a frequency dependent peak in Q^{-1} which mimics that of $\tan\delta$; the former indicates coupling of acoustic modes with central peak modes from dynamic PNR's, while the latter appears to be related to the relaxation of twin walls between 109°/71° domains.[39] In poled and depoled 0.955PZN-0.045PT, the patterns of variation of elastic and anelastic anomalies obtained from RUS are clearly dominated by ferroelastic aspects of rhombohedral ↔ tetragonal and tetragonal ↔ cubic phase transitions, but a memory effect from static PNR's was also revealed.[24]

Figure 1(a) shows the composition of the crystals used for the present study in relation to the location of the morphotropic phase boundary (MPB) at room temperature in PIN-PMN-PT, together with nearby compositions for which dielectric and Brillouin scattering data are already available. It includes values from the literature of T_m measured at 1 kHz for PIN, PMN and for samples with compositions close to the room temperature MPB in PIN-PT and PMN-PT. The value of T_c for PT is also given. Figure 1(b) shows the temperatures of dielectric anomalies measured at 1 and 10 kHz from Wang *et al.*[40] for poled ceramic samples with changing PMN/PT contents across the MPB in ternary ceramics with 0.36PIN. Anomalies near 430 K were interpreted as indicating the transition temperature, T_{rt}, for the $R3m$ ferroelectric (r) to $P4mm$ ferroelectric (t) transition, and values of T_m were taken to mark the $P4mm \leftrightarrow Pm\bar{3}m$ paraelectric (c) transition. The topology is typical of the central portion of phase diagrams for PMN-PT, PZN-PT, PIN-PT, and PZT ($Pb(Zr,Ti)O_3$), leaving aside discussion of the nature of the phase or phase mixture, which might be stable in the close vicinity of the vertical MPB itself (e.g., Refs. 41–48). Crystals of PIN-PMN-PT described below were expected to show the r ↔ t ↔ c sequence of the relatively PT-poor part of Figure 1(b). Table I gives transition temperatures from the literature determined for both single crystal and ceramic samples with the nearby compositions shown in Figure 1(a). These are generally lower than in Figure 1(b), but it is clear that the overall pattern of structural evolution is reproducible between samples prepared in different ways.

The $R3m \leftrightarrow P4mm$ transition is necessarily first order in character (not a group/subgroup relationship) and involves some temperature interval of coexisting phases. The $P4mm \leftrightarrow Pm\bar{3}m$ transition in samples of PMN-PT, which are close to or on the PT-rich side of the MPB is

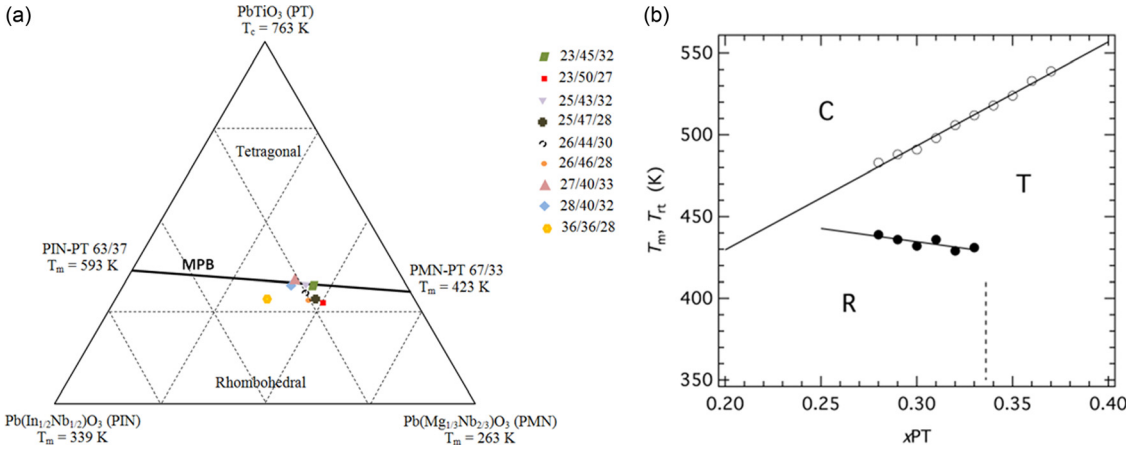

FIG. 1. (a) Schematic phase diagram for the PMN-PIN-PT ternary system. The MPB composition at room temperature traces an almost linear region between PIMNT 0/67/33 and PIMNT 63/0/37.[49] Data points mark the composition of the sample used in the present study and nearby compositions described in the literature. (b) Data for T_m and T_{rt} determined from anomalies in dielectric permittivity measured at 1 and 10 kHz for ceramics with ternary compositions and 0.36PIN from Wang *et al.*[40] C, T, and R mark stability fields of cubic, tetragonal, and rhombohedral structures without consideration of a possible stability field for the monoclinic structure.

TABLE I. Reported transition temperatures of selected PIN-PMN-PT samples with compositions on the PT-poor side of the MPB, as identified by anomalies in dielectric permittivity measured at 1 kHz. Transition temperatures estimated from elasticity data in the present study and from the literature are included for comparison; for these, values of T_m are given in brackets.

Composition PIN/PMN/PT	Direction of poling	T_{rt} (K)	T_{ro} (K)	T_{ot} (K)	T_m (K)
~26-36/32-46/28-32 (~0.29PT) (Ref. 54)	$[001]_c$[a]	393			443
26/46/28 (Ref. 53)	$[001]_c$	389			438
26/46/28 (Ref. 53)	unpoled				481
*x*PIN(1-*x*-*y*)PMN*y*PT $x > 0.25$–0.35 $y > 0.30$–0.32 (Ref. 55)	$[001]_c$	378–396[b]			456–434[b]
23/50/27(Ref. 56)	$[001]_c$	390			433
28/40/32 (Ref. 33)	$[001]_c$	384[c]			453[c]
28/40/32 (Ref. 57)	$[001]_c$	392			465
27/40/33 (Ref. 58)	$[001]_c$	369			470
23/45/32 (Ref. 59)	$[-101]_c$	383	391		444
25/47/28 (Ref. 60)	$[011]_c$		400	408	443
*x*PIN(1-*x*-*y*)PMN*y*PT[d] (Ref. 61) $x > 0.25$–0.35 $y > 0.30$–0.32	$[111]_c$	396			439
36/36/28, poled ceramic (Ref. 40)		439			483
25/43/32 (Ref. 49) unpoled ceramic					486
26/44/30 (RUS, heating)	$[001]_c$	≤~383			~463 (T_m = 462)
26/44/30 (RUS, cooling)	$[001]_c$				~439 (T_m = 457)
26/46/28 (RUS, heating)	$[111]_c$	402			~430 (T_m = 446)
26/46/28 (Ref. 53) (Brillouin)	$[001]_c$	389			423 (T_m = 438)

[a]Two poling directions were specified for this sample and it has been assumed here that the data were given for $[001]_c$; the measurement frequency was not specified.
[b]Compositions were not fully specified; data reproduced here are for crystals which were rhombohedral at room temperature.
[c]Transition temperatures identified by anomalies in thermal expansion.
[d]Composition not fully specified; data reproduced here are for a crystal which was rhombohedral at room temperature. Measurement frequency also not specified.

weakly first order, as in PT itself (e.g., Refs. 50 and 51). Small discontinuities in lattice parameter data also appear to be present at the same transition in PIN-PT.[48] It is weakly first order and close to tricritical on the $PbZrO_3$-rich side of the MPB in single crystals of PZT.[52] There are few data for the thermodynamic character of this transition in the ternary phases, but a thermal expansion study of a single crystal of 0.28PIN-0.40PMN-0.32PT poled along $[001]_c$ has revealed a discontinuity in strain at 453 K, again signifying weakly first order behavior.[33]

Properties obtained by RUS are for lower measuring frequencies and involve averaging over longer length scales than for the other principal source of elasticity data, namely Brillouin spectroscopy. Brillouin data have been reported for a $[001]_c$-poled single crystal with composition 0.26PIN-0.46PMN-0.28PT,[53] which is nominally the same composition as the $[111]_c$-poled crystal used here. These show steep changes in the frequency shift of a LA mode at ~389 and ~423 K, which are presumed to correspond to T_{rt} and T_c, respectively. Brillouin spectra from the unpoled crystal showed a broad minimum at ~413 K during heating and at ~385 K during cooling. The Burns temperature was estimated to be ~593 K, on the basis of a decrease in width of a central peak in the Brillouin spectra, but this is well below the temperature at which the onset of softening occurs (>600 K). T_m at 1 kHz was ~436 K for the poled crystal and ~481 K for the unpoled crystal. The Vogel-Fulcher freezing temperature for the unpoled crystal was found to be 454 K.

II. EXPERIMENTAL METHODS

A. Sample preparation and characterization

The two PIN-PMN-PT samples used for RUS in the current study were cut from a single crystal grown using the vertical Bridgman technique.[62] Their compositions were determined by quantitative energy dispersive spectroscopy in a Hitachi 4300 field-emission scanning electron microscope. One crystal, with dimensions ~5 × 4 × 3 mm^3 and composition 0.26PIN-0.44PMN-0.30PT was poled along the $[001]_c$

direction. In terms of the description of domain engineered crystals of Davis *et al.*,[9] this would be expected to be 4R (four rhombohedral twin domains with polar directions parallel to $[111]_c$, $[11\text{-}1]_c$, $[1\text{-}11]_c$, and $[1\text{-}1\text{-}1]_c$ at room temperature). The second crystal, with dimensions $\sim 5 \times 5 \times 1$ mm^3 and composition 0.26PIN-0.46PMN-0.28PT, was poled along $[111]_c$, corresponding to 1R (one rhombohedral twin with polar direction parallel to $[111]_c$). Poling was achieved by applying a dc bias field of 10 kV/cm at room temperature.

Piezoresponse force microscopy of a different piece of the same original (unpoled) crystal, with composition 0.29PIN-0.44PMN-0.27PT, revealed a labyrinthine domain pattern with domain widths of 50–150 nm, comparable to that observed in other relaxor ferroelectrics.[63] An $[001]_c$ poled sample was confirmed to contain a single, essentially homogeneous domain (in terms of only the vertical direction, maybe 4R), at least on a scale of $4 \times 4\ \mu$m^2, by the same method.

Following the RUS experiments, the crystals were repoled and their temperature dependent dielectric properties measured using an Agilent E4980 LCR meter connected to a customized heating furnace. The $[001]_c$-poled crystal had two sharp peaks in dielectric permittivity (measured at 1 kHz) at 374 and 456 K and a broad maximum at 462 K in data collected during heating, and a single broad maximum at 457 K during cooling. Similar anomalies occurred at 401, 431, and 446 K during heating of the $[111]_c$-poled crystal and at 442 K during cooling.

B. Resonant ultrasound spectroscopy

The underlying principles of the RUS method have been set out in detail elsewhere (e.g., Refs. 64 and 65). Equipment used routinely for data collection in the temperature interval ~5–1400 K in Cambridge has been described by McKnight *et al.* (e.g., Refs. 66 and 67) and in a number of subsequent studies of elastic and anelastic phenomena (including Refs. 34, 35, 37, 38, and 68). In combination, the frequencies of resonances of a sample with known shape allow the determination of single crystal elastic moduli or, in the case of a polycrystalline sample, of the bulk and shear moduli. Even if this complete analysis is not attempted, the frequency, f, of individual resonances can be used to follow the temperature dependence of the elastic properties. There is some single elastic modulus or combination of moduli associated with each resonance mode that scales with f^2. The full width at half of the maximum height of resonance peaks, Δf, depends on anelastic relaxations[65] and is typically used to determine values of the inverse mechanical quality factor as

$$Q^{-1} = \Delta f / f. \quad (1)$$

Room temperature RUS spectra were collected from the PIN-PMN-PT $[001]_c$-poled and $[111]_c$-poled crystals in the frequency range 0.05–2 MHz with the samples in four different orientations to observe as many resonances as possible. Spectra were then collected in a helium flow cryostat, starting with a cooling sequence from room temperature to 10 K in 30 K steps, with 15 min for thermal equilibration at each temperature. 65 000 and 130 000 data points through the frequency range 0.05–1.2 MHz were collected at each temperature for the $[001]_c$- and $[111]_c$-poled crystals, respectively. Spectra containing 65 000 data points in the frequency range 0.05–1.2 MHz were collected at high temperatures during heating and cooling sequences between 295 K and 700 K in 5 K steps, with a 15 min settle time allowed before data collection at each temperature. This was followed by a new set of measurements at low temperatures following the same sequence as before, with 65 000 data points per spectrum in the ranges 0.1–1.2 MHz and 0.05–1.2 MHz, for the now depoled $[001]_c$ and $[111]_c$ crystals, respectively.

Precision and accuracy of quoted temperatures from the low temperature instrument are better than ± 1 K. Temperatures from the high temperature instrument were corrected by comparison with a calibration of the $\beta \leftrightarrow \alpha$ transition at 846 K in quartz and are believed to have uncertainties of $\sim \pm 1$ K.

All the spectra were transferred to the software package IGOR PRO (Wavemetrics) for detailed analysis. This involved determining the frequency, f, and FWHM, Δf, of prominent resonance modes by fitting with an asymmetric Lorentzian function, an approach analogous to that described by Schreuer *et al.*[69]

III. RESULTS

A. $[001]_c$-poled sample: Raw spectra

Broad resonance peaks can be observed in RUS spectra from the $[001]_c$-poled crystal of 0.26PIN-0.44PMN-0.30PT

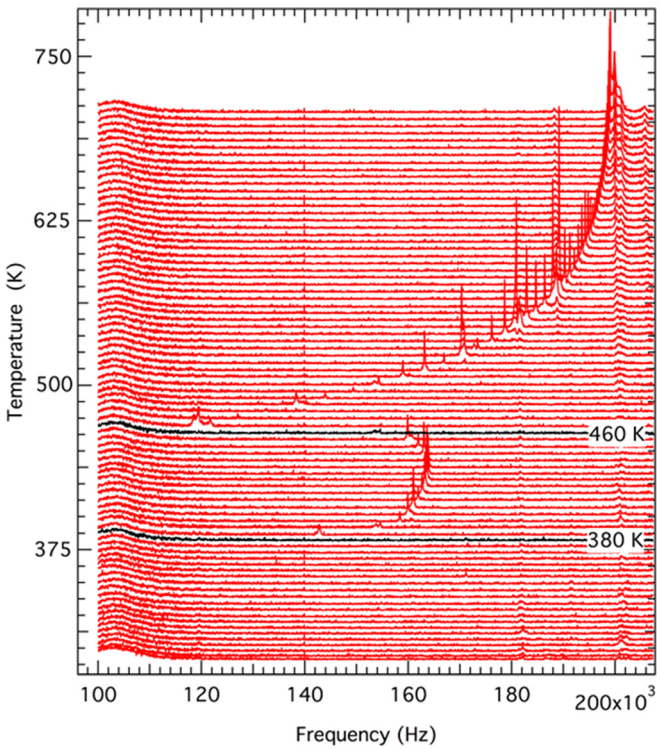

FIG. 2. Segments of RUS spectra for $[001]_c$-poled 0.26PIN-0.44PMN-0.30PT crystal collected during heating from 290 K to 700 K. The y-axis is amplitude but the individual spectra have been displaced in proportion to the temperature at which they were collected and the axis label is shown as temperature. Weak peaks which do not vary with temperature are from alumina rods of the high temperature instrument.

at low temperatures, though these are hard to discern below ~100 K. With increasing temperature, they all show frequency lowering, indicative of elastic softening. As shown in Figure 2, resonance peaks cannot be resolved in spectra from the high temperature instrument until they appear at ~385 K. This is followed by stiffening and then steep softening between ~460 and 465 K. These two temperatures are presumed to correspond with r → t and t → c transitions. Spectra collected at temperatures within the stability field of the cubic phase contain a large number of sharp resonances, which show stiffening with further heating.

Spectra collected during cooling from 700 K down to 465 K are indistinguishable from those collected during heating, apart from a very slight upward shift in frequency of the peak positions. Weak peaks can still be discerned in spectra collected down to 441 K, but then are not resolvable in spectra collected from 436 K down to room temperature. In the low temperature instrument, samples rest directly on the transducers, providing the best possibility for detecting weak resonances, and some peaks are visible in spectra collected in the low temperature run subsequent to their cooling from ~700 K.

Quantitative results are given in Figure 3, which shows the temperature dependence of f^2 and Q^{-1} during heating of the initially $[001]_c$-poled crystal and subsequent cooling of the depoled crystal. These data were obtained from peaks which had frequencies of ~196, ~253, ~291, ~304, ~318, and ~544 kHz at 290 K.

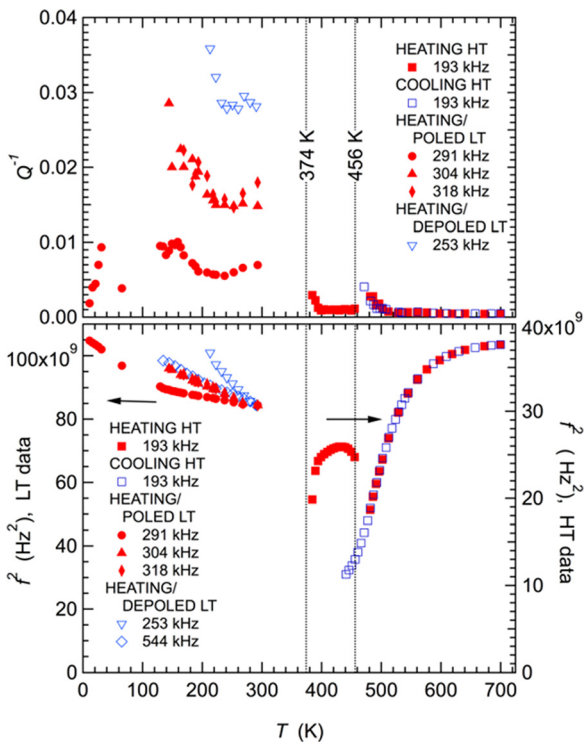

FIG. 3. Results from the analysis of RUS spectra from $[001]_c$-poled PIN-PMN-PT (HT = above room temperature and LT = below room temperature). f^2 data from low temperatures are plotted with respect to the left axis while data from high temperatures are plotted with respect to the right axis. Frequencies given in the caption refer to approximate values at room temperature.

1. Poled crystal

There are substantial variations of Q^{-1} in the stability field of the rhombohedral structures. Between ~10 and ~30 K, weak peaks gave relatively low values of Q^{-1}, but peaks were not easily detectable in the interval ~30–130 K, indicating $Q^{-1} > \sim 0.03$. Above ~130 K, there is a trend of softening with increasing temperature, with relatively high Q^{-1} (~0.01–0.02). Because of the lower signal to noise ratio of spectra from the high temperature instrument, these resonance peaks could not be followed as $T \rightarrow T_{rt}$ from below. The r → t transition appears to be defined by an abrupt reduction in Q^{-1} to values typical of materials with low acoustic loss ($Q^{-1} < \sim 0.001$). The last temperature at which peaks could not be detected was 379 K, and the first at which they could be detected was 384 K. This would put T_{rt} at ~383 K or below, which is just above the value of 374 K assumed from the peak in permittivity for the same crystal. It should be noted that f^2 values for different peaks shown in Figure 3 for temperatures below 300 K were scaled so as to have the same value at room temperature, and that it was not possible to link them to specific peaks observed in the high temperature spectra.

With increasing temperature in the stability field of the tetragonal phase, the elastic constants first stiffened and then softened as $T \rightarrow T_c$. The t → c transition is clearly defined by the abrupt reduction in elastic stiffness which occurred between 460 and 465 K, which is just above the value of $T_c = 456$ K taken from the peak in dielectric permittivity. Peaks in the spectrum collected at 460 K are barely detectable, however, in comparison with the strong sharp resonance peaks observed at 465 K, and the two sets of data are not incompatible. The cubic phase is then characterized by steep stiffening from 465 K up to at least 700 K. It was not possible to fit peaks in spectra collected between 460 and 481 K, but the values of Q^{-1} in this temperature range would clearly have been part of the distinct tail present at the onset of the stability field of the cubic phase. Q^{-1} reduces to approximately constant low values above ~510 K.

2. Depoled crystal

Data from spectra collected during cooling from ~700 K reveal the elastic and anelastic properties of the depoled crystal. Steep softening seen as $T \rightarrow T_c$ is the same during cooling as observed during heating, as is the increase in Q^{-1} below ~510 K. The last spectrum in which a weak resonance peak could be resolved was collected at 441 K, and the first in which resonance peaks could no longer be detected was collected at 436 K. On the basis of these weak peaks, the softening trend of the cubic phase extends to at least 441 K, i.e., ~20 K below the value of T_c, which is clearly marked in the heating data.

No data are shown in Figure 3 for cooling between 440 K and room temperature because peaks were not visible in the spectra. The few data it was possible to obtain below room temperature indicate the same pattern of stiffening with falling temperature as seen in the data for the poled crystal, but with higher values of Q^{-1} (~0.03). The marked increase in Q^{-1} below ~130 K is also repeated in data from the depoled crystal but it was not possible to resolve peaks in

spectra at the lowest temperatures to indicate whether the dissipation then reduced again below ~50 K.

B. $[111]_c$-poled sample: Raw spectra

Figure 4 shows spectra collected on heating from low to high temperatures from the $[111]_c$-poled crystal. The overall pattern of softening and stiffening is qualitatively similar to that shown by the spectra in Figure 2 from the $[001]_c$-poled crystal. There is a marked difference in the resonance peaks below T_c, however. These are effectively absent from spectra in the intermediate temperature interval expected to relate to the stability field of the tetragonal structure, and they are noticeably sharper and stronger in spectra from the rhombohedral phase.

As with the $[001]_c$-poled crystal, resonance peaks were not detected in spectra collected using the high temperature instrument during cooling between the temperature at which they were last resolved, perhaps near 420 K, and room temperature. They were clearly present in spectra from the low temperature instrument, however, and showed a pattern of stiffening with falling temperature.

Variations of f^2 and Q^{-1} from peaks with different frequencies at room temperature in these spectra and in spectra collected during subsequent cooling are shown in Figure 5. Note that, for display purposes in this figure, absolute values of the frequencies have been rescaled so that the data for each peak overlap at ~700 K, from the high temperature instrument, and at ~10 K from the low temperature instrument. This is because it was not possible to match individual peaks between high and low temperatures.

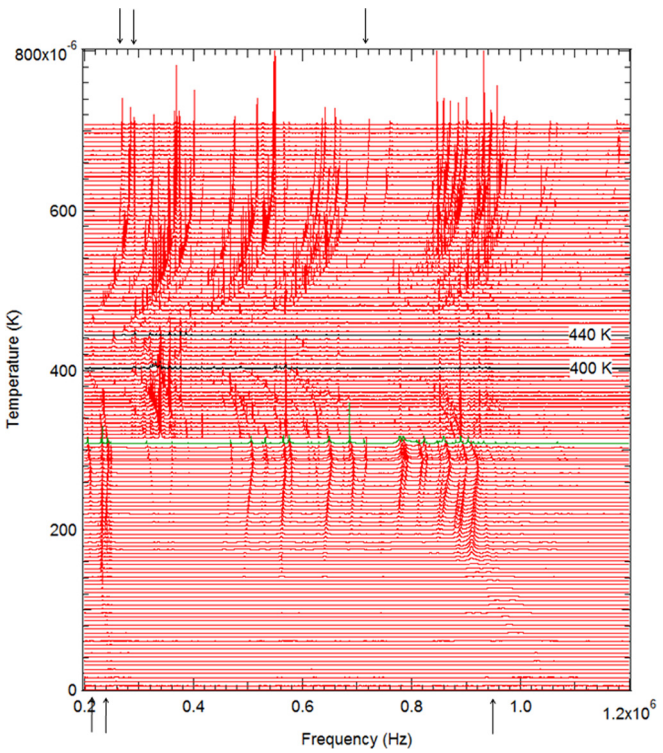

FIG. 4. Stack of RUS spectra for $[111]_c$-poled 0.26PIN-0.46PMN-0.28PT crystal. The change from high-temperature to low-temperature instruments is marked with a green line. The y-axis is amplitude but the spectra have been displaced in proportion to the temperature at which they were collected and the axis label is shown as temperature. Weak peaks which do not vary with temperature are from alumina rods of the high temperature instrument. Arrows indicate some of the peaks that were used to obtain f and Q^{-1}.

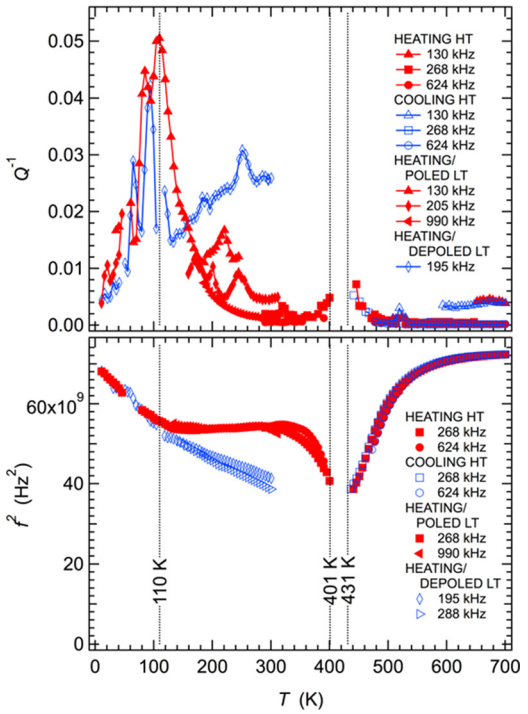

FIG. 5. Results from the analysis of RUS spectra from $[111]_c$-poled PIN-PMN-PT (HT = above room temperature and LT = below room temperature). No peaks were resolved between ~400 K and ~440 K in spectra collected during both heating and cooling and between ~420 and room temperature during cooling. Frequencies given in the caption refer to values at room temperature.

1. Poled crystal

In the lowest temperature range, the decrease in f^2 is approximately linear with increasing temperature from ~10 to ~130 K. There is then a plateau between 150 K and 310 K. This is followed by steep softening, the disappearance of resonance peaks, and then steep stiffening. The last temperature at which resonance peaks could be detected was 400 K, and the first temperature at which they could be detected again was hard to define but was somewhere in the range 427–436 K. These mark the limits of the presumed stability field of the tetragonal phase, and values of $T_{rt} = 402$ and $T_c = \sim 430$ K are assumed. In the stability field of the cubic phase and for much of the stability field of the rhombohedral phase, the values of Q^{-1} remain low, indicating low dissipation. A broad Debye-like peak in Q^{-1} occurs between ~70 and ~135 K, with its maximum at ~110 K. There is a premonitory increase in Q^{-1} as $T \rightarrow T_{rt}$ from ~380 K and an equivalent tail above T_c which reaches baseline values by ~480 K.

2. Depoled crystal

The form of evolution of f^2 and Q^{-1} in the stability field of the cubic phase of the initially $[111]_c$-poled crystal appears to be fully reversible during cooling from 700 K to ~440 K. There is a slight upward shift of the resonance frequencies in comparison with data from the heating sequence, as found also for the $[001]_c$ crystal, but, because the peaks in

spectra collected near 430 K are weak, it has not been possible to conclude whether there is also a hysteresis in T_c. Data from resonances in spectra from the low temperature instrument show approximately linear stiffening with falling temperature and a slight break in slope at ~120 K, rather than the plateau seen in data from the poled crystal. Values of Q^{-1} are higher (0.02–0.03) between ~160 and 300 K than for the poled crystal (0.005-0.015). An additional small peak in Q^{-1} appears to be present near 250 K. The Debye-like peak in dissipation is closely similar to that observed for the poled crystal apart from being displaced to a slightly lower temperature, with its peak at ~90 K rather than ~110 K.

IV. DISCUSSION

In PMN-PT and PZN-PT, relaxor characteristics increase with increasing PMN or PZN content away from the MPB (see, Ref. 18 and many references therein). The typical pattern of dielectric permittivity from a poled crystal has a single broad peak at T_m, which varies with frequency and a second anomaly, which is independent of measuring frequency, at a lower temperature, T_d. Values of T_d increase as the PT content is increased towards the MPB, as shown in Figure 9 of Ref. 15. The former defines the typical relaxor freezing behaviour while the latter marks the temperature at which depoling occurs on heating and defines the transition from ferroelectric to relaxor properties, T_{RF} (e.g., Refs. 19, 50, and 70–72). Although not always stated explicitly in the literature, T_d, T_{RF}, and T_c appear to mark the same point in the structural evolution as seen from slightly different points of view. The only exception seems to be for the data of Zekria *et al.*,[51] which give values of T_c from birefringence measurements on PMN-PT in the vicinity of T_m rather than T_d/T_{RF}.[73]

With increasing PT content, the difference between $T_d/T_{RF}/T_c$ and T_m diminishes; for example, it is ~20 K at 0.77PMN-0.23PT[30] and ~8 K at 0.67PMN-0.33PT.[29] In the compilation of data for PMN-PT, Davis[73] shows the difference as going to zero at a composition which corresponds with that of the MPB. Kim *et al.*[53] gave this difference as ~15 K from heating of a $[001]_c$-poled crystal of 0.26PIN-0.46PMN-0.28PT. Of the two crystals used here, the $[001]_c$ crystal has the higher PT-content and is, therefore, closer to the MPB than the $[111]_c$ crystal. From the dielectric permittivity measurements, the difference between T_d and T_m is 6 K for the former and 15 K for the latter. Although the nominal composition of the present $[001]_c$-poled crystal and that of Kim *et al.*[53] is the same, there are clearly some differences in exact behaviour, which may depend on sample preparation. In addition, Kim *et al.*[53] found that T_m at 1 kHz shifts up from ~438 K (poled) to ~478 K (unpoled) and that the second anomaly disappears for the unpoled crystal, implying that there is also an increase in relaxor characteristics which is not related simply to composition (their Fig. 2).

Patterns of evolution of elastic constants and acoustic dissipation from RUS measurements mirror the ferroelectric/relaxor transition behaviour from the perspective of ferroelasticity. The ferroelectric phases show features in common with the results from phases with improper ferroelastic phase transitions due to octahedral tilting in perovskites. Coupling of the order parameter with macroscopic spontaneous strains causes renormalisation of the elastic constants, typically as a stepwise softening at the transition point, and the development of ferroelastic twin walls gives rise to a steep increase in attenuation. The relaxor phases should be more similar to PMN, in which the influence of the PNR's is seen overtly in a continuous variation of elastic constants, first softening with falling temperature, then passing through a broad minimum in the temperature interval of freezing, and then recovering as temperature reduces further. This is accompanied by low background levels of acoustic loss at high temperatures, a steep increase in Q^{-1} in the freezing interval, followed by a decline back to lower values as $T \rightarrow 0$ K. Variations in both f^2 and Q^{-1} show some frequency dependence in the freezing interval. Broadly, the evolution of poled crystals of PIN-PMN-PT is comparable with that of the classical improper ferroelastic perovskites, i.e., reflecting the influence of macroscopic phase transitions, while the evolution of the depoled crystals is similar to that of PMN, i.e., reflecting control by the PNR's. Properties of the cubic phase are strongly influenced by contributions from the PNR's.

A. Softening in the stability field of the cubic structure

Elastic softening within the stability field of the cubic phase as $T \rightarrow T_c$ occurs over a temperature interval of at least 250 K for the two crystals used in the present study and at least 350 K for the 0.26PMN-0.46PMN-0.28PT crystal used by Kim *et al.*[53] In PMN, the onset of this softening coincides with T_B (~630 K) defined with respect to changes in other physical properties, such as thermal expansion and refractive index (e.g., Refs. 28, 39, and 74). An alternative criterion that has been applied for identifying the Burns temperature is a change in line width of phonon peaks in Brillouin spectra, which gives $T_B \approx 593$ K for 0.26PMN-0.46PMN-0.28PT (Ref. 53) and ~700 K for 0.65PIN-0.35PT.[75] These estimates of T_B are well below the onset of softening, however, and even for PMN, the same increase in linewidth occurs at ~450 K (e.g., Ref. 76) rather than 630 K. Similarly, for 0.93PZN-0.07PT, the onset of softening is ~100–200 K above the onset of line broadening of LA- and TA-phonon peaks.[77] In the RUS data for PMN,[39] there were no signs of any elastic or anelastic anomalies which could be interpreted as signifying T_B, apart from the onset of softening. On this basis, it is concluded that the Burns temperature for 0.26PIN-0.44PMN-0.30PT and 0.26PIN-0.46PMN-0.28PT is slightly above the maximum temperature (700 K) applied in the present study. This is comparable with $T_B \approx 750$ K, as defined by the onset of elastic softening for (1-x)PMN-xPT with $x = 0.31$, 0.35, and 0.55.[78]

Mechanical resonance modes of small samples in an RUS experiment are dominated by shearing. In the stability field of the cubic phase, the square of each resonance frequency will scale mainly with C_{44}, $\frac{1}{2}(C_{11} - C_{12})$ or a mixture of the two, and with only relatively small contributions from the bulk modulus. For the present sample, as in PMN,[39] all the resonances in spectra collected at high temperatures show the same pattern of softening, implying that all the acoustic modes are being affected in essentially the same

way, without any specific symmetry constraints. The softening mechanism is probably by coupling of acoustic phonons with dynamic components of the PNR's, which also give rise to central peaks (e.g., Refs. 39, and 78–83).

Premonitory changes in Q^{-1} from the low values of the cubic phase at high temperatures occur in an interval of ~40–50 K above T_c for both poled and depoled crystals (Figs. 3 and 5). The onset of acoustic loss at ~300 kHz is thus ~35–50 K above the value of T_m (at 1 kHz). The onset of dielectric loss also occurs in about this temperature range in ternary crystals (e.g., 100 kHz data in Fig. 3 of Ref. 56 for 0.23PIN-0.50PMN-0.27PT), and the two effects are presumed to relate to the slowing down of PNR dynamics as the freezing interval is approached. Dielectric losses will depend primarily on 180° flipping, while the acoustic loss will depend primarily on local flipping between 71/109° orientations. The freezing process must involve both.

Apart from rather slight shifts in resonance frequencies, there appears to be no sign of significant hysteresis in the elastic properties of the cubic phase during heating and cooling sequences for the $[001]_c$ and $[111]_c$ crystals. This is in contrast with the hysteresis in PZN-PT, which indicated that static poling of PNR's can persist above T_c.[24] However, there does appear to be a hysteresis of ~20 K in the t ↔ c transition temperature for the $[001]_c$-poled crystal. Elastic softening during cooling of this crystal continues down to at least ~441 K, and the transition point is presumably marked by the loss of resonance peaks in spectra collected below this. Some hysteresis is inevitable at a first order transition but the difference, which is essentially the same as has been reported by Kim *et al.*,[53] re-emphasises the dominance of relaxor behaviour in the absence of a bias field.

B. Rhombohedral ↔ tetragonal and tetragonal ↔ cubic transitions

In Brillouin spectra from crystals with ternary and binary compositions close to the MPB, r → t and t → c transitions are clearly defined during heating by steep changes in frequency shift of LA phonon peaks (e.g., $[001]_c$-poled 0.26PMN-0.46PMN-0.28PT;[53] unpoled 0.65PIN-0.35PT;[75] unpoled 0.67PMN-0.33PT;[84] and unpoled 0.69PMN-0.31PT.[78]). Diffraction and elasticity data are not usually both available from a single sample but in the case of $[001]_c$-poled 0.955PZN-0.045PT, at least, a sharp minimum in a shear elastic constant from RUS measurements, which was probably $\frac{1}{2}(C_{11} - C_{12})$, coincides within experimental error with T_c from neutron diffraction (Ref. 24). Although the transition points for the samples described here are somewhat obscured by the associated increases in acoustic loss, there seems little doubt that the elastic and anelastic anomalies near 380 and 460 K in RUS spectra from the $[001]_c$-poled crystal correspond to the r ↔ t and t ↔ c structural transitions, therefore.

In the case of an improper ferroelastic phase transition which is weakly first order and close to tricritical, the expected pattern of softening for most of the single crystal elastic constants would be a step at T_c, followed by a nonlinear recovery, as shown in Figure 3 of Carpenter *et al.*[39] The pattern of f^2 variations seen in Figure 3 for the $[001]_c$-poled crystal can be understood in terms of this step and nonlinear recovery below T_c, combined with PNR-related softening above T_c. It thus appears to be entirely consistent with the ferroelectric to relaxor transition, which has been characterized mainly on the basis of dielectric data in the literature (e.g., Refs. 15, 18, 29, 71, and 72). From the perspective of strain and elasticity, the transition is from improper ferroelastic to relaxor.

The pattern of softening as T_{rt} is approached from below ($[111]_c$-poling, Fig. 5) and from above ($[001]_c$-poling, Fig. 3) is indistinguishable from what is seen at an equivalent first order transition without a group-subgroup symmetry relationship (*Imma* ↔ *I*4/*mcm*) in $SrZrO_3$.[34] The width of any two-phase field is not known but tails in Q^{-1} on both sides of T_{rt} (Figs. 3 and 5) are also similar to what is seen in $SrZrO_3$. The loss mechanism could be from mobile interfaces between coexisting phases or from premonitory fluctuations/clustering in a single phase material. Either way, it is clear that the elastic property variations can be understood as being due to ferroelastic relaxations which would be expected of a normal, as opposed to relaxor, ferroelectric.

During cooling of 0.67PMN-0.33PT, the form of the abrupt change in Brillouin frequency shift of the LA phonon remains unchanged,[84] implying that the relaxor → ferroelectric transition is much the same as the ferroelectric → relaxor transition. In the heating sequence of unpoled 0.26PMN-0.46PMN-0.28PT, however, the two steep changes from the poled crystal are replaced by a single broad minimum approximately midway between T_{rt} and T_c.[53] This pattern is more similar to that seen in PMN (e.g., Ref. 39), and also occurs in both LA (C_{11}) and TA (C_{44}) Brillouin frequency shifts from unpoled 0.955PZN-0.045PT (Ref. 82) and 0.93PZN-0.07PT.[77] In the ternary phases and some binary phases, therefore, the relaxor → ferroelectric transition is not the same as ferroelectric → relaxor in relation to the development of relatively coarse twin domains without the influence of an external field. The broad minimum occurs in resonance frequencies from RUS spectra collected during cooling from high temperatures for 0.955PZN-0.045PT, but there are still discernable breaks in slope at T_{rt} and T_c to show that the transitions occur even if relatively coarse ferroelectric/ferroelastic twins do not develop.[24]

The microstructure of unpoled 0.29PIN-0.44PMN-0.27PT at room temperature consists of a labyrinthine domain pattern[63] but the evidence of acoustic loss presented here indicates that at least some part of this relaxor microstructure has ferroelastic properties. In other words, it contains interfaces which move in response to an applied stress with relaxation times in the vicinity of $\sim 10^{-6}$ s and which become pinned below ~110 K.

C. Twin- and defect-related acoustic losses

Abrupt disappearance of resonance peaks has been described as superattenuation in the case of the r ↔ c transition in $LaAlO_3$, where it was due to the presence of ferroelastic twin walls in the rhombohedral phase (e.g., Refs. 37 and 85). Acoustic losses observed here in the stability fields of both ferroelectric phases at RUS frequencies can be understood similarly in terms of the mobility of ferroelastic twin walls

between 90° domains of the tetragonal structure and between 71/109° domains of the rhombohedral structure. $[111]_c$ poling of PIN-PMN-PT on the rhombohedral side of the MPB should produce a crystal containing, nominally, a single rhombohedral domain with no ferroelectric or ferroelastic twin walls. This would be expected to have the lowest acoustic loss, and observed Q^{-1} values are ~0.001–0.004 for the temperature interval ~300–380 K (Fig. 5). $[001]_c$ poling should produce a crystal nominally with four differently oriented rhombohedral domains, and a higher density twin walls. This is reflected in the higher values of Q^{-1}, 0.006–0.015, in the same temperature interval (Fig. 3). Heating this crystal into the stability field of the tetragonal phase must have resulted in a reduction in the number of twin walls, as indicated by the reduction of Q^{-1} values to ~0.001. Finally, unpoled crystals should have the highest density of twin walls and should show the highest acoustic losses, as is indeed observed, with $Q^{-1} \approx 0.02$–0.03 for both crystals in the temperature interval 200–300 K (Figs. 3 and 5).

Between ~50 and ~150 K, there are one or more Debye-like peaks in Q^{-1} for both crystals in their poled and depoled states. This can be accounted for by thermally activated strain-relaxation processes with characteristic relaxation times,

$$\tau = \tau_0 \exp(E_a/RT), \tag{2}$$

such that $\omega\tau = 1$ at the temperature, T_m, for which Q^{-1} reaches a maximum value, Q_m^{-1}. Here, ω $(= 2\pi f)$ is the angular frequency of the applied stress. A single Debye peak measured as a function of temperature at approximately constant frequency can be described by (from Refs. 86–88)

$$Q^{-1}(T) = Q_m^{-1}\left[\cosh\left\{\frac{E_a}{Rr_2(\beta)}\left(\frac{1}{T}-\frac{1}{T_m}\right)\right\}\right]^{-1}, \tag{3}$$

E_a is the activation energy and $r_2(\beta)$ is a width parameter which arises from a spread in relaxation times for the dissipation process. Fits to two peaks with the most complete set of data points from the $[111]_c$ crystal are shown in Figure 6. They have $E_a/Rr_2(\beta)$, Q_m^{-1} and T_m values of 730 K ($E_a/r_2(\beta) = 6.1$ kJ mol^{-1} = 0.063 eV), 0.044, 107 K and 1500 K ($E_a/r_2(\beta) = 12.5$ kJ mol^{-1} = 0.13 eV), 0.033, 92 K for the poled and depoled states, respectively. If the dissipation involves a single relaxation time, the value of β is 0 and the value of $r_2(\beta)$ is 1. The frequency, f, of the resonance peaks from which the Q^{-1} data were obtained was near 230 kHz, and rewriting Eq. (2) as $f = f_o \exp(-E_a/RT)$, then gives attempt frequency, f_o, values of $\sim 2 \times 10^8$ and $\sim 3 \times 10^{12}$ Hz, respectively. These are all clearly approximate values, and there is a strong correlation, in particular, between E_a and f_o. If there is a Gaussian spread of relaxation times, as specified by the value of β, the values of E_a and f_o will be larger. Nevertheless, they are within range of typical values obtained from dielectric spectroscopy data relating to the Vogel-Fulcher freezing process. For example, Kim *et al.*[53] reported $E_a/k_B = 610$ K and $f_o = 4.6 \times 10^{12}$ Hz for 0.26PIN-0.46PMN-0.28PT.

Dielectric and acoustic losses above the Vogel-Fulcher temperature of a relaxor arise by a collective freezing process, which involves a wide spectrum of relaxation times. The Debye-like peaks in Q^{-1} at low temperatures observed here are more typical of the freezing process for local displacements of individual defects under stress. By comparison with the typical pattern of acoustic losses associated with ferroelastic phase transitions, such as in $LaAlO_3$ (e.g., Refs. 37, 89, and 90), the most likely cause of the Debye peak near ~110 K might be considered to be pinning of the ferroelastic twin walls. Piezoelectric measurements provide independent evidence that the mobility of twin walls in PMN-PT ceramics at 1 Hz reduces with falling temperature at least down to ~120 K (Ref. 91). An increase in acoustic dissipation has been observed below ~200 K in 0.955PZN-0.045PT,[24] and freezing of macroscopic domain wall motion has previously been reported for PZN-PT near 243 K.[92] However, the $[111]_c$-poled crystal should in principle have no twin walls, while the depoled crystal should have a large number, and both display loss peaks. What appears to be the case is that there are multiple local loss mechanisms. Assuming that the poled samples contain no ferroelastic twin walls would imply that the peak at ~110 K corresponds to the final pinning of some other defect, such as the boundaries between PNR's. The peak at ~90 K from the depoled sample could be from local displacements of the twin walls. The kinetic parameters obtained by fitting have values which match with those for the Vogel-Fulcher freezing process at higher temperatures, so the local mechanism must involve essentially the same style of energy barrier. This contrasts with the pinning process for ferroelastic needle twins in $LaAlO_3$ and for ferroelastic/ferroelectric twin walls in $SrBi_2Ta_2O_9$, for example, in which a much higher activation energy, ~0.9 eV, indicates a dominating role for oxygen vacancies (e.g., Refs. 89 and 93).

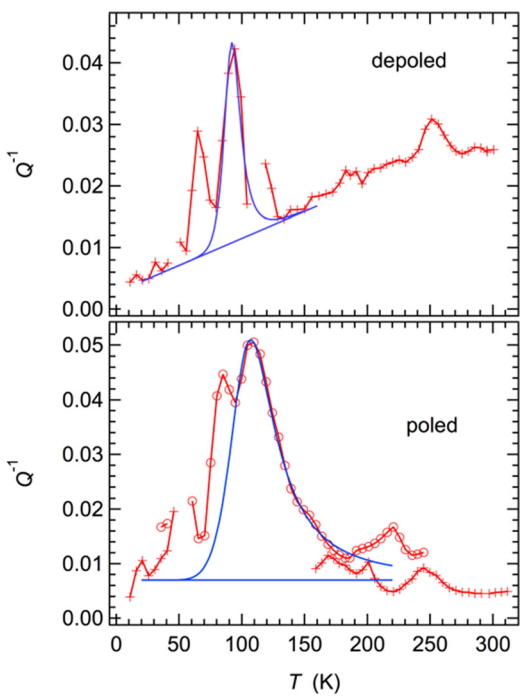

FIG. 6. Fits of Eq. (3) to individual Debye-like peaks in Q^{-1} from the $[111]_c$ crystal. Straight lines correspond to estimates of the baseline in each case.

Taking the Debye loss peaks at face value as implying some variety of local freezing processes also has implications for the overall elastic properties of PIN-PMN-PT crystals. The Debye equations give[94]

$$Q^{-1} = \Delta \frac{\omega\tau}{1+\omega^2\tau^2}, \quad (4)$$

and, in the case of a standard linear solid,

$$\Delta = \frac{C_U - C_R}{C_R} \quad (\text{for}(C_U - C_R) \ll C_R), \quad (5)$$

where C_U is the relevant elastic constant for the unrelaxed state and C_R the elastic constant of the relaxed state. At $\omega\tau = 1$, $Q^{-1} = Q_m^{-1}$ but because Eq. (1) was used with amplitude data rather than intensity data, the experimental values have to be reduced by a factor of $\sim\sqrt{3}$ (Eq. (6) below). Using $Q_m^{-1} = 0.019$ and 0.025, then gives $\Delta = 0.04$ and 0.05. In other words, above the freezing point each of these extrinsic relaxation processes contributes ~4%–5% softening. Their freezing is responsible for most, if not all, of the stiffening which is evident below ~100 K for both crystals in Figures 3 and 5. If, as appears to be the case, there are multiple loss processes, the total contribution of the relaxations could be ~10%–20%, say, for measurements made in the vicinity of 1 MHz and under the low stress conditions of RUS. By the same argument, it is expected that there would also be changes in piezoelectric properties when extrinsic contributions freeze out at low temperatures, as has been attributed to the effect on twin wall mobility in PZT and PMN-PT (e.g., Refs. 91 and 95).

These patterns of acoustic loss correlate to some extent with patterns of dielectric loss. For example, dielectric losses down to ~120 K measured at 1 and 10 kHz for poled crystals of 0.72PMN-0.28PT are lower for poled than for depoled crystals,[96] as would be expected if the main loss mechanism is motion of ferroelectric twin walls and/or PNR boundaries in an effectively viscous matrix. However, an increase in loss below ~120 K for poled crystals was not observed in unpoled crystals and was attributed to pinning of point defects to twin walls between macrodomains that remained. This was accompanied by elastic stiffening and a decrease in the piezoelectric coefficient d_{31}. On the other hand, Priya *et al.*[97] observed a frequency dependent peak in tanδ for PMN-PT, with a maximum near 100 K when measured at 100 kHz, which they attributed to "structural irregularities (or fractal clusters of lower symmetry) inside of normal micron-sized domains." This seems more akin to the origin of the acoustic losses observed in the present study. The precise origin remains unclear, however, particularly as similar behaviour is observed in crystals, which are supposed to be "normal" rather than relaxor ferroelectrics.[98]

Experience of twin wall mediated loss behaviour in purely ferroelastic materials indicates that, in detail, different loss mechanisms may operate. At low frequencies (~1–100 Hz) and relatively high stresses (sufficient to give strains of 10^{-3}–10^{-5}), the dominant mechanisms in the case of $LaAlO_3$ appear to be the advance and retraction of the tips of needle domains and rotation of the walls out of their preferred crystallographic plane. The twin walls in $LaAlO_3$ interact with oxygen vacancies such that it may be necessary to exceed a critical stress before they start to move away from their pinned positions, however.[99] The relaxation time characteristics also do not appear to match up with those obtained at low stress and higher frequencies, and with Carpenter *et al.*[37] suggesting that there must be some more local bowing mechanism for the twin walls. For thin walls, this would most likely occur by nucleation of ledges and their subsequent migration parallel to the length of the walls,[90] as reproduced also in simulations of twin wall motion.[100]

In order to produce a more comprehensive picture of mechanical loss mechanisms in PIN-PMN-PT, it will be necessary to explore the influence of stress and measuring frequency more systematically to produce anelasticity maps of the type which have been suggested for $LaAlO_3$ (see, Refs. 37 and 90). It is anticipated that the dominant loss mechanism for poled crystals at high measuring frequencies and low stress will be due to motion of ledges/kinks of the twin walls. For unpoled crystals, the same mechanism could apply to twin walls which might be present on a much smaller length scale within the PNR's. Thicker twin walls or boundaries between PNR's would not be subject to the same pinning force[101] and should be able to migrate more freely at low levels of stress.

D. Mechanical quality factor, Q_m

As recently reviewed by Zhang and Li,[6] it can be important to control mechanical loss characteristics of relaxor ferroelectric single crystals used in device applications. For example, low Q (relatively high mechanical loss) is desirable in medical imaging transducers, whereas high Q (low mechanical loss) is required for high power sonar transducers. The loss data of interest are expressed as Q_m in tables of properties of selected samples of PMN-PT, PMN-PZT, PIN-PMN-PT, and Mn-doped PIN-PMN-PT, in Zhang and Li.[6] The authors pointed out that values of this mechanical quality factor are higher in single domain crystals than multidomain engineered crystals (e.g., Refs. 5 and 10), they increase with increasing domain size[102] and they vary with crystallographic orientation of the poling[5] (see also Refs. 3, 8, and 103). For example, Q_m is ~200 for a $[001]_c$-poled 4R (multidomain) crystal, ~800 for $[001]_c$-poled 1T (single domain) crystal, and ~1000 for a $[111]_c$-poled 1R (single domain) crystal of PIN-PMN-PT.[5] Observed values also vary with proximity to the MPB, being higher for crystals with relatively lower PT contents, away from the MPB,[5] and the same pattern is seen also for ceramic samples.[40] Clearly, the dominant factors are the mobility and density of ferroelastic twin walls but there appear to be rather few data for the effects of temperature, particularly through the phase transitions. Zhang and Li[6] showed steep reductions in Q_m for differently poled PIN-PMN-PT crystals with increasing temperature towards the r ↔ t transition point and Zhang *et al.*[5] showed equivalent patterns followed by abrupt increases at T_{rt} for Mn-doped PIN-PMN-PT.

Data presented here indicate that RUS provides an effective technique for exploring mechanical loss characteristics

at both low and high temperatures, but direct comparison of absolute values of Q must be made with some regard to the precise experimental conditions. First, values of Q from the widths of amplitude peaks in the RUS signal differ by a factor of $\sim\sqrt{3}$ from those obtained from intensity in other measurements, or from $\tan\delta_m$, where δ_m is the phase angle in the response to an applied dynamic stress. For small damping,

$$\tan\delta_m \approx \frac{1}{\sqrt{3}}\frac{\Delta f}{f} = \frac{1}{\sqrt{3}}Q^{-1} \quad (6)$$

(see Refs. 104 and 105). To facilitate comparison with data in the literature, data for Q^{-1} in Figures 3 and 5 have been replotted as $Q_m = \sqrt{3}Q$ in Figure 7. Second, Zhang *et al.*[5] reported that there is a strong dependence of Q_m on the maximum dynamic strain imposed in the experimental determination, with values of ~200–1000 at maximum strains of $\sim10^{-4}$ and <100 at maximum strains of $\sim10^{-3}$. It is not known precisely what the maximum strain might be during mechanical resonance of a 3–5 mm parallelepiped in an RUS experiment, but Walsh *et al.*[106] made an estimate of $\sim10^{-7}$. Finally, domain wall movement is generally thermally activated, with some characteristic relaxation time, which will vary with temperature such as given in Eq. (2). The extent of twin wall movement and, hence, of acoustic loss will be frequency dependent. Here, data are for frequencies of ~0.1–1 MHz, which overlap with measurements of Zhang and co-workers made using an impedance analyzer in the vicinity of 0.1 kHz (e.g., Refs. 102 and 103).

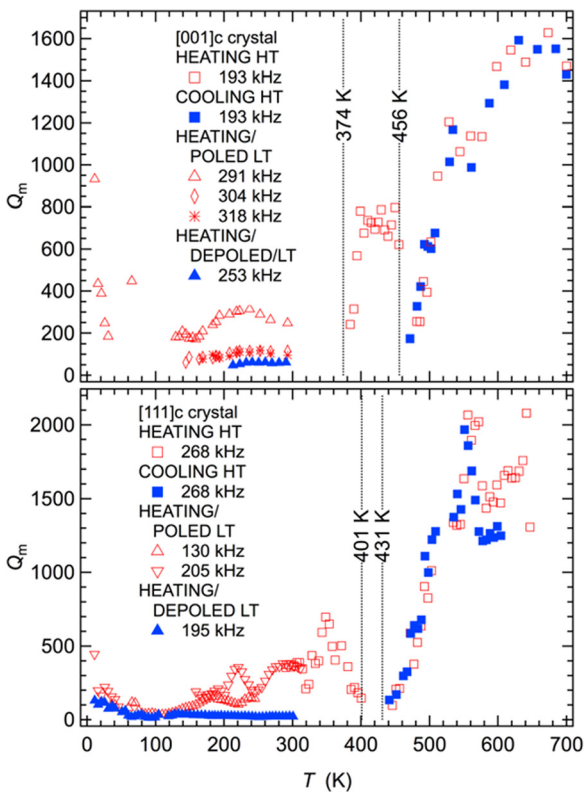

FIG. 7. Variation of mechanical quality factor, Q_m, with temperature for $[001]_c$-, $[111]_c$-poled crystals and after depoling. (HT = above room temperature and LT = below room temperature).

Figure 7 shows variations of Q_m between ~40 and ~2000 for $[001]_c$-poled, $[111]_c$-poled and depoled samples measured from resonances in the frequency range ~0.1–0.3 MHz. Absolute values of Q from the high temperature instrument appear to be modified by the influence of the alumina rods through which the acoustic signal must travel to and from the sample and have, therefore, been scaled to match with values measured at room temperature, where the sample sits directly between the transducers. The highest values of Q_m were obtained for crystals in the stability field of the cubic structure and are presumed to provide a measure of low intrinsic loss, combined with extrinsic factors such as motion of cracks, impurities, dislocations, etc. The next highest values are for the $[111]_c$-poled sample in the stability field of the rhombohedral structure (1R) and for the $[001]_c$-poled sample in the stability field of the tetragonal structure (perhaps 1T in the notation of Ref. 9). Reduction of Q_m values to ~400 and ~800, respectively, reflects additional loss mechanisms, which could be due to rotation of the polarisation direction within macroscopic twin domains, displacement of any remaining twin walls, displacements of boundaries between polarised PNR's and the matrix in which they lie, or motion of locally misoriented regions associated with other defects.

The steep reduction of Q_m as $T \rightarrow T_c$ from above correlates with the steep softening, which has been attributed to the influence of dynamic PNR's. This acoustic loss further emphasises the fact that local correlations of electric dipoles must be accompanied by local ferroelastic shear strains. Similar reductions occur as $T \rightarrow T_{rt}$ from below in the $[111]_c$-poled crystal and from above in the $[001]_c$-poled crystal, implying that fluctuations or clusters of locally differently strained states also occur in anticipation of the r ↔ t transition. Low (<~50) values of Q_m for the depoled crystals are consistent with loss mechanisms due to the mobility of multiple twin walls and/or interfaces of unpolarised PNR's. Freezing processes which occur below ~150 K lead to recovery of Q_m up to at least ~400, and manipulation of these to higher temperature, say by the addition of impurities, might add to the methods evaluated by Sherlock *et al.*[103] for engineering the characteristic acoustic properties of PIN-PMN-PT single crystals.

Two generalisations can be drawn from comparison with the new insights provided here and data from the literature. From the low-temperature results, it appears that there are multiple acoustic loss mechanisms for which the activation energy landscape is not dissimilar from that encountered in the Vogel-Fulcher freezing process for electric dipoles. From the result of Zhang *et al.*[5] for the effect of changing stress, there must be differences in the strength of pinning of the microstructure in these materials. Both highlight, again, the importance of ferroelastic aspects of relaxor ferroelectric properties that are exploited in device applications.

E. Influence of static PNR's below T_c and T_{rt}

As set out in the introduction above, a generalised view of relaxor-ferroelectric behaviour is of some combination of the limiting behaviour of a conventional ferroelectric such as PT and of a relaxor such as PMN. The soft optic mode of the former becomes modified by the freezing behaviour of

dynamic PNR's of the latter. At intermediate compositions in binary systems, such as PMN-PT, the freezing interval defined by maxima in the dielectric permittivity overlaps with T_c for the discrete t↔c transition. This should be reflected in the elastic and anelastic properties, which are also different for the two limiting cases. The ferroelectric order parameter, q, couples with volume and tetragonal or rhombohedral shear strains, e, in a linear-quadratic manner, λeq^2, which does not give rise to softening as the ferroelectric transition point is approached from above. The observed softening below T_B is, therefore, one of the most readily distinguishable influences of dynamic PNR's. Any fluctuations in the cubic phase ahead of the phase transition are likely also to cause softening but the temperature range over, which it occurs in perovskites is much greater for ferroelectric transitions than for ferroelastic transitions. For example, the softening interval is ~300 K in PIN-PMN-PT (this study,[53]), PMN,[39] and PZN-PT (see Refs. 74 and 107), and ~250 K for $BaTiO_3$ (Ref. 108) but less than ~50 K for $BaCeO_3$,[35] $SrTiO_3$,[109] $LaAlO_3$,[37] $SrZrO_3$,[34] and $KMnF_3$.[38]

The influence of PNR's on elastic properties below the freezing interval can be seen in differences between heating of poled crystals and cooling of depoled crystals. The characteristic pattern for freezing of the PNR's is shown by PMN and is a rounded minimum in the elastic constants through the freezing interval followed by elastic stiffening, with acoustic losses closely resembling the dielectric losses.[39] This rounded minimum in elastic properties was seen by Kim *et al.*[53] for cooling of unpoled PIN-PMN-PT but their poled sample gave abrupt changes more typical of discrete phase transitions.

Additional information from the present study relates to the acoustic loss, which is low for the poled crystals in the stability fields of their respective tetragonal and rhombohedral stability fields. The poling must reduce acoustic losses both from twin walls of the ordered ferroelectric structure and from the PNR's, consistent with the view that the static PNR's are themselves poled (e.g., Refs. 20–23). This poling of the PNR's can then account for the memory effect in cubic PZN-PT,[24] the restoration of a tetragonal phase with low acoustic losses from a rhombohedral crystal poled along $[001]_c$ (this study) and the stability field of an orthorhombic phase when the poling is along $[110]_c$ (e.g., Refs. 11, 55, 59, 60 and 110–115). Davis[18] compared some of these effects with the influence of internal bias fields due to the presence of defects.[18] It is clear that the structural and domain states of relaxor ferroelectrics can be manipulated specifically through controlled poling of the PNR's not only by the choice of orientation but, as shown by Lu *et al.*,[111] also by the strength of the poling field.

V. CONCLUSIONS

Variations of the elastic and anelastic properties of single crystals of PIN-PMN-PT during heating and cooling are consistent with changes in the twin domain configurations shown in Figures 8 and 9 for $[001]_c$ and $[111]_c$ poled states, respectively.

(i) In the stability field of the cubic phase, marked softening with falling temperature is understood in terms of coupling of acoustic modes with local fluctuations due to dynamical PNR's. The temperature interval of this softening is substantially greater than occurs ahead of improper ferroelastic transitions in other perovskites. Acoustic loss attributed to slowing down of the PNR dynamics occurs in a temperature interval of ~50 K above T_c when measured at frequencies of ~0.1–1 MHz and low applied stress.

(ii) Cubic ↔ rhombohedral and tetragonal ↔ rhombohedral transitions are marked, in particular, by abrupt changes of acoustic loss associated with changes in the density of ferroelastic twin walls. Unpoled crystals have strong acoustic losses which are probably due also to contributions from mobile interfaces between static PNR's or between PNR's and the matrix.

(iii) The pattern of losses in poled PIN-PMN-PT crystals is comparable with what is observed for twin walls in ferroelastic perovskites, with evidence for freezing of twin wall motion in the vicinity of 100 K (at frequencies in the vicinity of 0.2 MHz).

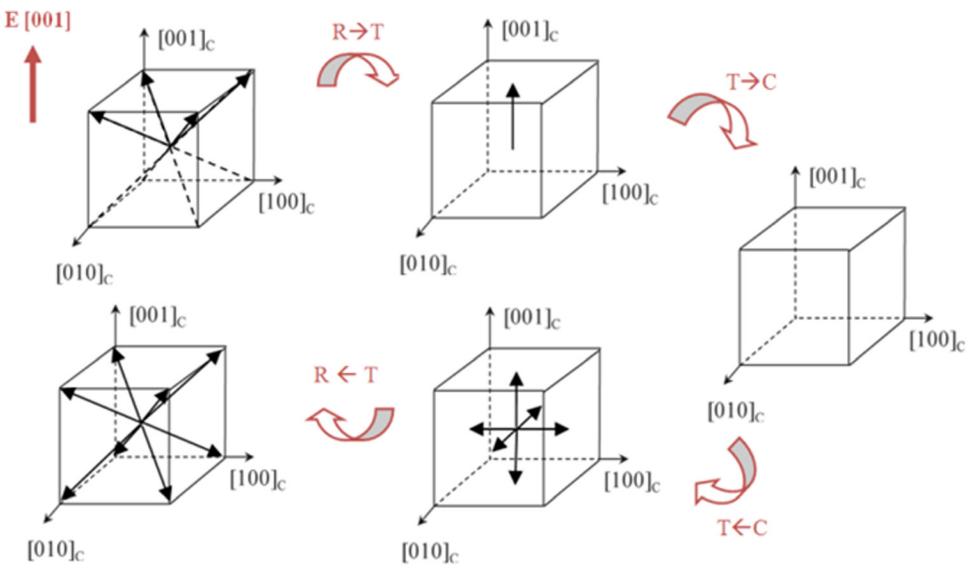

FIG. 8. Schematic polarization and depolarization sequence for $[001]_c$-poled crystal, with polarization directions represented by arrows.

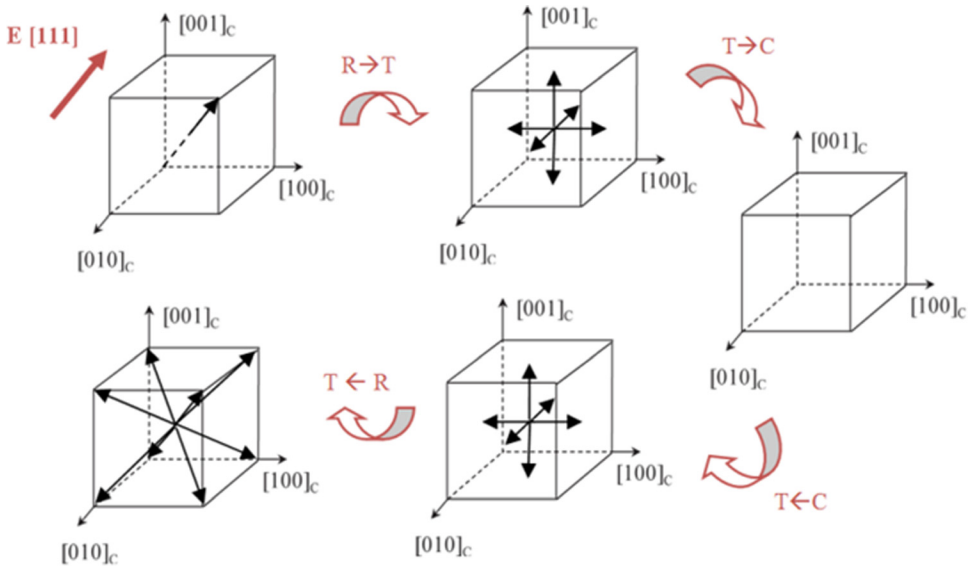

FIG. 9. Schematic polarization and depolarization sequence for $[111]_c$-poled crystal with polarization directions represented by arrows.

(iv) Evidence has been found for additional Debye-like freezing processes at low temperatures, and the activation energy landscape for these appears to be similar to that which operates during Vogel-Fulcher freezing of PNR's at higher temperatures. Each of the low temperature freezing/pinning processes contributes changes of ~4%–5% to the magnitudes of shear elastic constants, implying that the measured elastic properties at room temperature include substantial softening due to extrinsic effects.

(v) While the elastic and anelastic properties of twinned ferroelectric crystals are dominated by conventional effects of strain/order parameter coupling and twin wall mobility, the influence of static, poled PNR's within the twinned crystals can be seen in memory effects such that their orientation acts as a field to give preferred orientations of macroscopic domains.

(vi) The ferroelectric transitions take place in crystals which are heterogeneous due to the presence of static PNR's. Poling characteristics of the PNR's might be exploited as an additional means of engineering crystals to have desirable acoustic loss properties. For example, poling at different temperatures will set the orientation of the PNR's in a manner that is not reset by subsequent cooling. In this context, RUS provides a quick and effective means of characterizing the influence of different poling and chemistry on the mechanical quality factor Q_m.

ACKNOWLEDGMENTS

RUS facilities in Cambridge were established with support from the Natural Environment Research Council of Great Britain (NE/B505738/1 and NE/F017081/1). One of us (G.F.N.) wishes to thank E. K. H. Salje for co-advising his internship.

[1]Y. Hosono and Y. Yamashita, J. Electroceram. **17**, 577 (2006).
[2]P. Sun *et al.*, IEEE Trans. Ultrason. Ferroelectr. Freq. Control **56**, 2760 (2009).
[3]J. L. Luo *et al.*, IEEE Int Ultr Symp Proc (2009), p. 968.
[4]F. Li *et al.*, Adv. Funct. Mater. **21**, 2118 (2011).
[5]S. Zhang *et al.*, J. Cryst. Growth **318**, 846 (2011).
[6]S. Zhang and F. Li, J. Appl. Phys. **111**, 031301 (2012).
[7]W. Dong, P. Finkel, A. Amin, and C. S. Lynch, Proc. SPIE **8343**, 834308 (2012).
[8]S. Zhang and T. R. Shrout, IEEE Trans. Ultrason. Ferroelectr. Freq. Control **57**, 2138 (2010).
[9]M. Davis, D. Damjanovic, D. Hayem, and N. Setter, J. Appl. Phys. **98**, 014102 (2005).
[10]S. J. Zhang *et al.*, Appl. Phys. Lett. **94**, 162906 (2009).
[11]E. Sun, S. Zhang, J. Luo, T. R. Shrou, and W. Cao, Appl. Phys. Lett. **97**, 032902 (2010).
[12]G. Shirane *et al.*, Phys. Rev. B **2**, 155 (1970).
[13]G. Burns and F. H. Dacol, Solid. State. Commun. **48**, 853 (1983).
[14]D. Viehland *et al.*, J. Appl. Phys. **68**, 2916 (1990).
[15]A. Bokov and Z.-G. Ye, J. Mater. Sci. **41**, 31 (2006).
[16]R. A. Cowley *et al.*, Adv. Phys. **60**, 229 (2011).
[17]K. Hirota, S. Wakimoto, and D. E. Cox, J. Phys. Soc. Jpn. **75**, 111006 (2006).
[18]M. Davis, J. Electroceram. **19**, 23 (2007).
[19]A. Bokov, H. Luo, and Z.-G. Ye, Mater. Sci. Eng. B **120**, 206 (2005).
[20]G. Xu, Z. Zhong, Y. Bing, Z.-G. Ye, and G. Shirane, Nature Mater. **5**, 134 (2006).
[21]G. Xu, Z. Zhong, H. Hiraka, and G. Shirane, Phys. Rev. B **70**, 174109 (2004).
[22]G. Y. Xu, P. M. Gehring, and G. Shirane, Phys. Rev. B **72**, 214106 (2005).
[23]G. Xu and P. M. Gehring, Phys. Rev. B **74**, 104110 (2006).
[24]S. M. Farnsworth *et al.*, Phys. Rev. B **84**, 174124 (2011).
[25]G. A. Smolenskii, N. K. Yushin, and S. I. Smirnov, Sov. Phys. Solid State **27**, 492 (1985).
[26]N. K. Yushin, E. P. Smirnova, and S. N. Dorogovtsev, Sov. Phys. Solid State **29**, 1693 (1987).
[27]S. N. Dorogovtsev and N. K. Yushin, Ferroelectrics **112**, 27 (1990).
[28]D. Viehland, S. Jang, M. Wuttig, and L. E. Cross, Philos. Mag. A **64**, 835 (1991).
[29]P. Bao, F. Yan, W. Li, Y. R. Dai, and H. M. Shen, Appl. Phys. Lett. **81**, 2059 (2002).
[30]F. Yan, P. Bao, and Y. Wang, Appl. Phys. Lett. **83**, 4384 (2003).
[31]M. Algueró, B. Jiménez, and L. Pardo, Appl. Phys. Lett. **87**, 082910 (2005).
[32]F. Yan *et al.*, J. Am. Ceram. Soc. **90**, 3167 (2007).
[33]P. Finkel, H. Robinson, J. Stace, and A. Amin, Appl. Phys. Lett. **97**, 122903 (2010).
[34]R. E. A. McKnight *et al.*, J. Phys. Condens. Matter **21**, 015901 (2009).
[35]Z. Zhang *et al.*, Phys. Rev. B **82**, 014113 (2010).
[36]M. A. Carpenter, E. C. Wiltshire, and C. J. Howard, Phase Trans. **83**, 703 (2010).
[37]M. A. Carpenter *et al.*, J. Phys. Condens. Matter **22**, 035405 (2010).
[38]M. A. Carpenter *et al.*, Phys. Rev. B **85**, 224430 (2012).

[39]M. A. Carpenter *et al.*, J. Phys. Condens. Matter **24**, 045902 (2012).
[40]D. Wang, M. Cao, and S. Zhang, J. Eur. Ceram. Soc. **32**, 433 (2012).
[41]B. Jaffe *et al.*, *Piezoelectrics Ceramics* (Academic Press, New York, 1971), 317 p.
[42]J. Kuwata, K. Uchino, and S. Nomura, Ferroelectrics **37**, 579 (1981).
[43]S. W. Choi *et al.*, Ferroelectrics **100**, 29 (1989).
[44]E. F. Alberta and A. S. Bhalla, J. Korean Phys. Soc. **32**, S1265 (1998).
[45]D. La-Orauttapong *et al.*, Phys. Rev. B **65**, 144101 (2002).
[46]B. Noheda *et al.*, Phys. Rev. B **63**, 014103 (2000).
[47]B. Noheda, D. E. Cox, G. Shirane, J. Gao, and Z. G. Ye, Phys. Rev. B **66**, 054104 (2002).
[48]C. Augier, M. PhamThi, H. Dammak, and P. Gaucher, J. Eur. Ceram. Soc. **25**, 2429 (2005).
[49]Y. Hosono and Y. Yamashita, Jpn. J. Appl. Phys., Part 1 **42**, 535 (2003).
[50]O. Noblanc, P. Gaucher, and G. Calvarin, J. Appl. Phys. **79**, 4291 (1996).
[51]D. Zekria *et al.*, J. Phys. Condens. Matter **17**, 1593 (2005).
[52]T. H. Kim, J.-H. Ko, S. Kojima, and A. A. Bokov, Appl. Phys. Lett. **100**, 082903 (2012).
[53]T. H. Kim *et al.*, J. Appl. Phys. **111**, 054103 (2012).
[54]W. Hackenberger, Z. Shujun, and T. R. Shrout, in *IEEE International Ultrasonics Symposium (IUS)* (2009), pp. 968–971.
[55]F. Li *et al.*, J. Appl. Phys. **109**, 014108 (2011).
[56]T. Fang, A. Konar, H. Xing, and D. Jena, Appl. Phys. Lett. **91**, 092109 (2007).
[57]G. Xu, K. Chen, D. Yang, and J. Li, Appl. Phys. Lett. **90**, 032901 (2007).
[58]X. Liu, S. Zhang, J. Luo, T. R. Shrout, and W. Cao, J. Appl. Phys. **106**, 074112 (2009).
[59]D. Liu *et al.*, J. Alloys Compd. **506**, 428 (2010).
[60]Y. Zhang *et al.*, J. Electron. Mater. **40**, 92–96 (2011).
[61]J. Gao *et al.*, J. Appl. Phys. **110**, 106101 (2011).
[62]X. Wang *et al.*, Ferroelectrics **401**, 173 (2010).
[63]Q. Li, Y. Liu, J. Schiemer, P. Smith, and Z. Li, Appl. Phys. Lett. **98**, 092908 (2011).
[64]A. Migliori and J. D. Meynard, Rev. Sci. Instrum. **76**, 121301 (2005).
[65]A. Migliori and J. L. Sarrao, *Resonant Ultrasound Spectroscopy* (Wiley, New York, 1997).
[66]R. E. A. McKnight *et al.*, Am. Mineral **92**, 1665 (2007).
[67]R. E. A. McKnight *et al.*, J. Phys. Condens. Matter **20**, 075229 (2008).
[68]Z. Zhang *et al.*, J. Phys. Condens. Matter **23**, 145401 (2011).
[69]J. Schreuer, C. Thybaut, M. Prestat, J. Stade, and S. Haussühl, in *2003 Proc. IEEE Ultrason. Symp.* (2003), pp. 196–199.
[70]M. L. Mulvihill, L. E. Cross, W. Cao, and K. Uchino, J. Am. Ceram. Soc. **80**, 1462 (1997).
[71]K. Fan, L. Kong, L. Zhang, and X. Yao, J. Mater. Sci. **34**, 6143 (1999).
[72]H. Wang *et al.*, Appl. Phys. Lett. **87**, 012904 (2005).
[73]M. Davis, Ph.D. dissertation no. 3513, Ecole polytechnic Federale de Lausanne, 2006.
[74]S. G. Lushnikov *et al.*, Phys. Rev. B **77**, 104122 (2008).
[75]V. Sivasubramanian, S. Tsukada, and S. Kojima, Jpn. J. Appl. Phys., Part 1 **47**, 7740 (2008).
[76]J.-H. Ko, D. H. Kim, S. Kojima, W. Chen, and Z.-G. Ye, J. Appl. Phys. **100**, 066106 (2006).
[77]S. Tsukada and S. Kojima, Phys. Rev. B **78**, 144106 (2008).
[78]J.-H. Ko, D. H. Kim, S. Tsukada, S. Kojima, and A. A. Bokov, Phys. Rev. B **82**, 104110 (2010).
[79]Y. Gorouya, Y. Tsujimi, M. Iwata, and T. Yagi, Appl. Phys. Lett. **83**, 1358 (2003).
[80]J. Toulouse *et al.*, Phys. Rev. B **72**, 184106 (2005).
[81]C. Stock, R. J. Birgeneau, S. Wakimoto, and J. S. Gard, J. Phys. Soc. Jpn. **74**, 3002 (2005).
[82]J.-H. Ko, D. H. Kim, and S. Kojima, Phys. Rev. B **77**, 104110 (2008).
[83]G. Xu, J. Wen, C. Stock, and P. M. Gehring, Nature Mater. **7**, 562 (2008).
[84]G. Shabbir and S. Kojima, Appl. Phys. Lett. **91**, 062911 (2007).
[85]M. A. Carpenter *et al.*, EOS Trans. Am. Geophys. Union **87**, abstract MR34A-01 (2006).
[86]M. Weller, G. Y. Li, J. X. Zhang, T. S. Kc, and J. Diehl, Acta Metall. **29**, 1047 (1981).
[87]R. Schaller, G. Fantozzi, and G. Gremaud, *Mechanical Spectroscopy Q-1 2001: With Applications to Materials Science* (2001).
[88]M. A. Carpenter, Phys. Rev. B **82**, 134123 (2010).
[89]R. J. Harrison, S. A. T. Redfern, and E. K. H. Salje, Phys. Rev. B **69**, 144101 (2004).
[90]M. A. Carpenter and Z. Zhang, Geophys. J. Int. **186**, 279 (2011).
[91]F. Li, S. Zhang, Z. Xu, and X. Wei, Appl. Phys. Lett. **96**, 192903 (2010).
[92]M. L. Mulvihill, L. E. Cross, and K. Uchino, J. Am. Ceram. Soc. **78**, 3345 (1995).
[93]F. Yan, X. Chen, P. Bao, Y. Wang, and J. Liu, J. Appl. Phys. **87**, 1453 (2000).
[94]A. S. Nowick and B. S. Berry, *Anelastic Relaxation in Crystalline Solids* (Academic, 1972).
[95]R. Gerson, J. Appl. Phys. **33**, 830 (1962).
[96]F. Wang *et al.*, J. Phys. D: Appl. Phys. **42**, 182001 (2009).
[97]S. Priya, D. Viehland, and K. Uchino, Appl. Phys. Lett. **80**, 4217 (2002).
[98]M. H. Lente *et al.*, Appl. Phys. Lett. **85**, 982 (2004).
[99]R. J. Harrison and S. A. T. Redfern, Phys. Earth Planet. Inter. **134**, 253 (2002).
[100]E. K. H. Salje, X. Ding, Z. Zhao, T. Lookman, and A. Saxena, Phys. Rev. B **83**, 104109 (2011).
[101]W. T. Lee *et al.*, Phys. Rev. B **73**, 214110 (2006).
[102]D. Lin *et al.*, J. Appl. Phys. **110**, 084110 (2011).
[103]N. P. Sherlock *et al.*, J. Appl. Phys. **107**, 074108 (2010).
[104]T. Lee, R. S. Lakes, and A. Lal, Rev. Sci. Instrum. **71**, 2855 (2000).
[105]R. S. Lakes, Rev. Sci. Instrum. **75**, 797 (2004).
[106]J. N. Walsh *et al.*, Phys. Earth Planet. Inter. **167**, 110 (2008).
[107]J.-H. Ko, T. Kim, K. Roleder, D. Rytz, and S. Koji, Phys. Rev. B **84**, 094123 (2011).
[108]J.-H. Ko *et al.*, Appl. Phys. Lett. **93**, 102905 (2008).
[109]M. A. Carpenter, Am. Mineral. **92**, 309 (2007).
[110]Y. Lu, D.-Y. Jeong, Z.-Y. Cheng, and Q. M. Zhang, Appl. Phys. Lett. **78**, 3109 (2001).
[111]Y. Lu, D.-Y. Jeong, Z.-Y. Cheng, T. Shrout, and Q. M. Zhang, Appl. Phys. Lett. **80**, 1918 (2002).
[112]Y. P. Guo *et al.*, J. Appl. Phys. **92**, 6134 (2002).
[113]Y. Guo, J. Phys. Condens. Matter **15**, L77 (2003).
[114]S. Zhang *et al.*, J. Appl. Phys. **102**, 114103 (2007).
[115]S. Zhang, S. Lee, D. Kim, H. Lee, and T. R. Shrout, J. Am. Ceram. Soc. **91**, 683 (2008).